Alpha-transfer reactions in light nuclei. II. (^{3}He, ^{7}Be) pickup reaction*

D. J. Pisano† and P. D. Parker
Wright Nuclear Structure Laboratory, Yale University, New Haven, Connecticut 06520
(Received 1 March 1976)

The (^{3}He, ^{7}Be) reaction has been studied at a laboratory energy of 25.5 MeV for ^{16}O and ^{24}Mg targets and at energies of 25.5, 27.0, and 29.0 MeV for a ^{12}C target. Angular distributions have been measured from $\theta_{lab} = 15°$ to 160° for transitions to low-lying states in the residual nuclei. The resulting angular distributions have been analyzed (1) using an exact-finite-range distorted-wave Born-approximation formalism including multistep processes and (2) using a Hauser-Feshbach compound-nuclear model. In general, the shapes of the forward angle (^{3}He, ^{7}Be) data are well described by the finite-range distorted-wave Born-approximation and finite-range coupled-channels Born-approximation calculations. The magnitude of the measured transition to the 1.63-MeV (2^+) state in ^{20}Ne is approximately 100 times larger than predicted by an SU_3 theory for a simple one-step transition, and this transition is shown to be an example in which a finite-range coupled-channels Born-approximation analysis is required. Arguments concerning the direct nature of the reaction process populating these states are discussed, and spectroscopic information is extracted.

[NUCLEAR REACTIONS ^{12}C, ^{16}O, ^{24}Mg(^{3}He, ^{7}Be), $E_{(^3He)} = 25.5$, 27.0, 29.0 MeV, measured $\sigma(E, \theta)$ Hauser-Feshbach and finite-range CCBA analysis, spectroscopic factors.]

I. INTRODUCTION

During the past several years, considerable experimental and theoretical effort has been devoted to the study of α-particle-transfer reactions on p-shell and sd-shell nuclei[1-9] in order to examine the importance of α-particle clustering in the structure of nuclei in this mass region. This information is important for our understanding of the nuclear structure of these nuclei and is also important in the analysis of the helium-burning[10,11] and silicon-burning[12,13] processes in nuclear astrophysics. Because of their greater experimental simplicity, most of the experiments have centered on the lithium-induced stripping reactions (^{6}Li, d) and (^{7}Li, t) with relatively few studies of related α pickup reactions.

These two types of reactions are quite complementary. In α-stripping reactions the extracted spectroscopic information relates the $[A_{g.s.} \otimes \alpha]$ configuration to one component of the configurations of the final states populated in the residual nucleus $(A+4)$. In α-pickup reactions, however, the spectroscopic information relates the components of the target ground-state configuration to the various $[(A-4)^* \otimes \alpha]$ configurations. In a simple, direct, one-step analysis the only overlap between these two types of reactions is in the ground-state to ground-state transition which can provide a very convenient interrelationship between these two sets of spectroscopic factors; in a multistep analysis, including inelastic processes, additional overlaps may be available.

Comparisons of the data from the (^{6}Li, d) and (^{7}Li, t) reactions indicate that the (^{7}Li, t) reaction is much more selective[1] in its population of the final states allowed under a simple α-cluster transfer picture. In view of this selectivity and in view of the strong, well established cluster structure of ^{7}Be,[14] the (^{3}He, ^{7}Be) reaction [the isospin mirror inverse of the (^{7}Li, t) reaction] should be a good α-pickup reaction to study for the extraction of spectroscopic information about the cluster configurations in various target nuclei.

Previously the only extensive work on the (^{3}He, ^{7}Be) reaction has been carried out by Détraz, Duhm, and Hafner,[15] first with 28- and 30-MeV ^{3}He beams and more recently[16] at incident energies up to 41 MeV. The work of Détraz has been analyzed in terms of a fixed-range distorted-wave Born-approximation (DWBA) theory[15] and has also been used to examine the reaction mechanism involved in this transfer reaction. The present study was undertaken to amplify this previous work (1) by measuring additional angular distributions at different incident beam energies to help elucidate the reaction mechanism involved, (2) by applying an exact-finite-range coupled-channel DWBA analysis to the analysis of these data, and (3) by extending these measurements to the ^{24}Mg(^{3}He, ^{7}Be)^{20}Ne reaction of interest to nuclear structure theorists[17] and to nuclear astrophysicists.[12]

II. EXPERIMENTAL PROCEDURE

The experimental measurements were performed using the Yale MP tandem accelerator in con-

junction with a duoplasmatron ion source and a lithium-vapor charge exchange medium for producing the negative ^{3}He ions. Reaction measurements were made in a standard 76-cm ORTEC scattering chamber with two independently movable detector mounts. The beam geometry in this chamber was defined by two entrance slits located 51 and 127 cm upstream from the target. These slits were 0.32 cm high and typically either 0.05 or 0.10 cm wide. After passing through the target the beam was collected in a magnetically shielded Faraday cup and integrated by a Rogers-type integrator,[18] calibrated with a known current source whose absolute accuracy was $<1\%$.

For most of the measurements, the ^{7}Be ions were detected using standard $\Delta E + E$ counter telescopes. Because of the low energy and high stopping power of the ^{7}Be ions, thin ($\lesssim$10-μm) Si(SB) ΔE detectors were used together with 50-μm Si(SB) E detectors. The particle identification system utilized pulse multipliers which formed the function $f(E, \Delta E) = \Delta E(E + E_0 + K\Delta E) \sim MZ^2$, where K and E_0 are adjustable constants and M and Z are the mass and charge of the detected ion.[19] (A storage oscilloscope was used as an aid in the adjustment of K and E_0 to optimize the separation of the desired particle species.) The separation of ^{7}Be is somewhat simpler than for other nearby nuclear species because both ^{6}Be and ^{8}Be are particle unstable and, therefore, well removed from the ^{7}Be locus. Gates were set on the ^{7}Be identifier signal and were used to route the linear $(E + \Delta E)$ signal to a quadrant of a 4096-channel Northern Scientific analyzer.

For the ^{12}C(^{3}He, ^{7}Be)^{8}Be reaction this method could not be used for angles $\theta_{lab} \gtrsim 100^\circ$ because the energies of the ^{7}Be particles are so low that they stop in our thinnest (6.8-μm) Si(SB) detector. Over the range $100^\circ \lesssim \theta_{lab} \lesssim 140^\circ$, however, the ^{7}Be groups populating the ^{8}Be ground state are the highest-energy particles stopping in the 6.8-μm detector so that they can be identified and measured by using this detector in conjunction with a 50-μm veto detector behind it. For angles beyond 140°, in this case, the energies of the ^{7}Be groups of interest are less than the energy of α particles stopping in the 6.8-μm detector, and this method is no longer effective.

Since the low-lying (429-keV) first excited state of ^{7}Be is particle stable, all groups corresponding to specific final states in the residual nuclei will be observed as doublets, corresponding to the detection of ^{7}Be ions in either their ground state or their 429-keV excited state. The necessity of resolving the two peaks in these doublets [so that separated cross sections could be measured for the (^{3}He, ^{7}Be$_{(0)}$) and (^{3}He, ^{7}Be$_{(1)}$) reactions] dictated the minimum energy resolution which could be tolerated, limiting the allowable angular spread and target thickness (as related to the energy losses of the emerging ^{7}Be particles), the primary sources of energy spread. In order to optimize this situation, the targets were tipped at 45° to the incident beam to increase their effective thickness to the beam and to decrease the ^{7}Be energy losses by reducing their path out of the target. At forward angles $\Delta\theta$ was typically restricted to $\lesssim 1.5^\circ$, but at backward angles $\theta \gtrsim 90^\circ$ where $dE/d\theta$ is less severe, $\Delta\theta$ could be increased to $\sim 4^\circ$. Measurements of the detector-slit geometry determined the experimental solid angle (typically, $\sim$1 msr at forward angles and $\sim$3 msr at $\theta_{lab} \gtrsim 100^\circ$) with an uncertainty of $\pm 3\%$.

Self-supporting 50- to 100-μg/cm^2 carbon foils were used for the ^{12}C(^{3}He, ^{7}Be)^{8}Be measurements. Oxygen targets were prepared by oxidizing 88-μg/cm^2 self-supporting nickel foils in air with a projection lamp. Similar nickel foils were also used as backing for the magnesium targets. [Nickel was chosen as a backing material because preliminary experiments had shown there to be negligible yields from Ni(^{3}He, ^{7}Be)Fe reactions.] Isotopically pure ^{24}Mg (>99.96%) was vacuum evaporated from a closed tantalum boat onto the nickel foils which were then transferred under vacuum to the scattering chamber in order to minimize oxidation of the magnesium. Furthermore, in order to reduce oxidation and minimize carbon buildup during bombardment, a 20-cm×20-cm liquid-nitrogen-cooled copper plate was installed inside the target chamber as close to the target as possible. At the end of the experiment, before exposure to air, the Mg+Ni target thickness was measured in the scattering chamber by observing the energy shift of the 5.48-MeV α-particle group from an ^{241}Am source when the target was placed between the source and a calibrated detector. Typical magnesium thicknesses were ≈ 65 μg/cm^2. Comparisons of measurements of the thicknesses of carbon foils and nickel foils using this technique and using an α gauge[20] showed agreement within the uncertainties of the individual measurements, typically $\lesssim \pm 10\%$.

III. EXPERIMENTAL RESULTS

Typical energy spectra for the (^{3}He, ^{7}Be) reaction on ^{12}C, ^{16}O, and ^{24}Mg targets are shown in Figs. 1–3. The energy resolution is typically 150–300 keV full width at half maximum (FWHM) and was determined primarily by target thickness and finite aperture effects as discussed above. Note that each state in the residual nucleus appears as a doublet due to the detection of ^{7}Be in

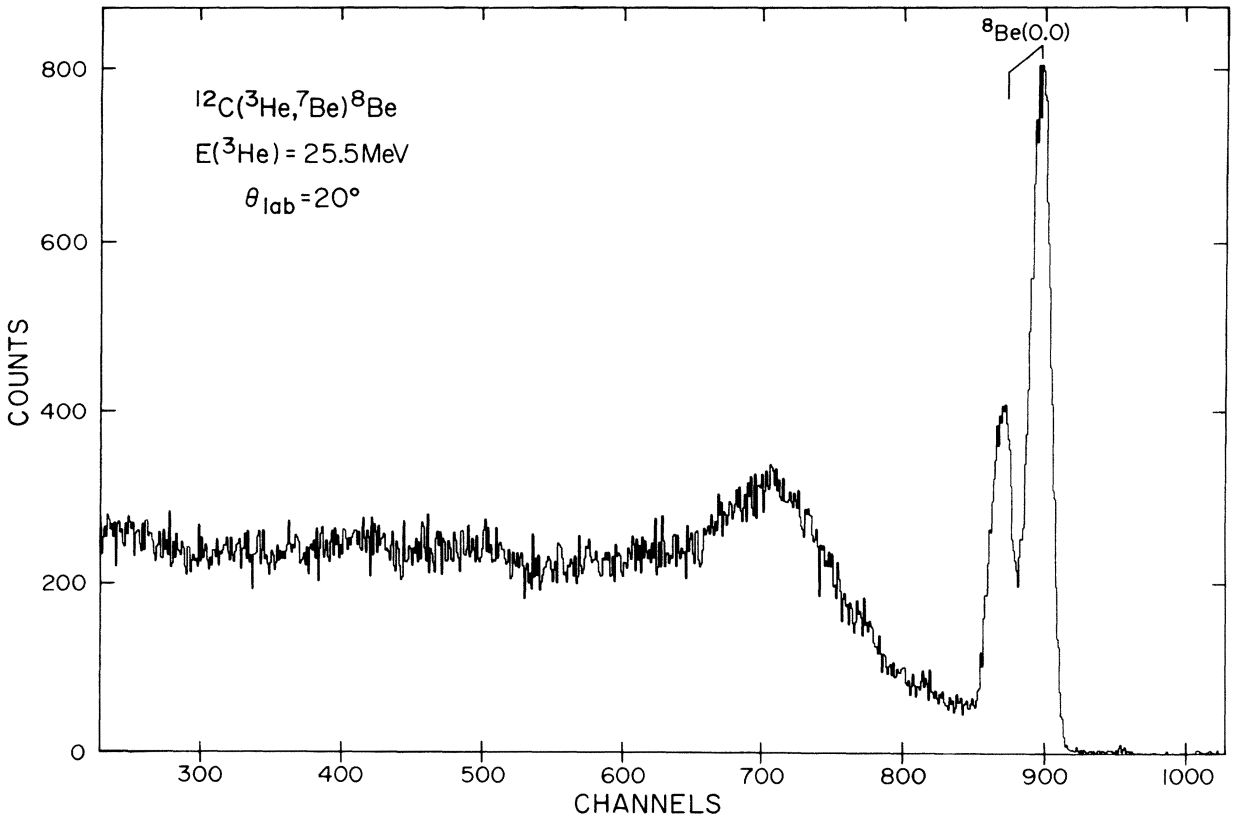

FIG. 1. Energy spectrum of ^{7}Be particles emitted in the $^{12}C(^3He,^7Be)^8Be$ reaction at a laboratory angle of 20° with a ^{3}He bombarding energy of 25.5 MeV. Note the doublet corresponding to detection of ^{7}Be in its ground and first excited states. The broad peak at channel 700 corresponds to the 2.9-MeV state in ^{8}Be.

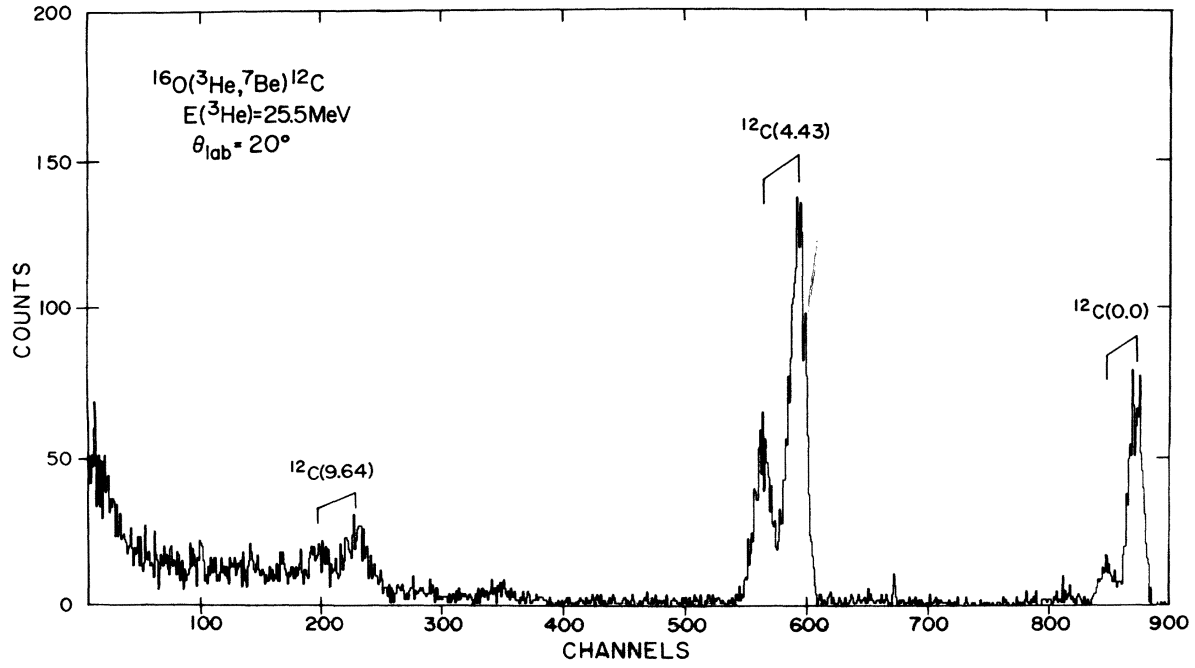

FIG. 2. Energy spectrum of ^{7}Be particles emitted in the $^{16}O(^3He,^7Be)^{12}C$ reaction at a laboratory angle 20° with a ^{3}He bombarding energy of 25.5 MeV. The doublets correspond to detection of ^{7}Be in its ground and first excited state.

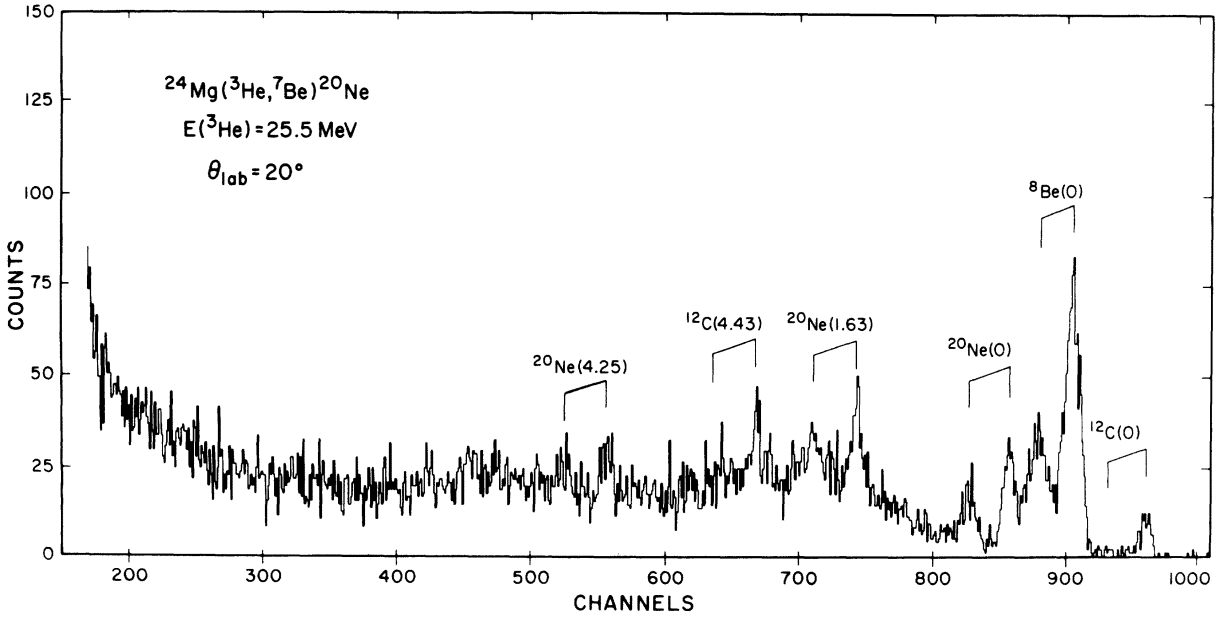

FIG. 3. Energy spectrum of ^{7}Be particles emitted at a laboratory angle of 20° in the (^{3}He,^{7}Be) reaction from a ^{24}Mg target. The doublets correspond to detection of ^{7}Be in its ground and first excited states. The peaks labeled ^{12}C and ^{8}Be are from reactions with the target contaminants ^{16}O and ^{12}C, respectively.

both its ground state and its 429-keV first excited state. In the measurements with the ^{24}Mg target the spectra are dominated by the yield from a small ^{12}C and ^{16}O contamination since the cross sections for the (^{3}He, ^{7}Be) reaction are as much as 100 times stronger for these nuclei than for ^{24}Mg.

Peak areas and cross sections were extracted from these spectra using a peak-fitting routine in which the groups corresponding to each state in the residual nucleus were fitted as a doublet (usually not nearly as well resolved as in these forward-angle spectra) with the separation between the two Gaussian components predetermined from kinematics and the energy calibration. The four remaining free parameters (two independent heights and widths) were even further restricted by the additional constraint that the widths of the two components be equal. These restrictions are physically quite reasonable and enable the fitting program to work efficiently with rapid convergence and to achieve good fits to the data. Angular distributions were extracted for the ^{8}Be ground state and the low-lying 0^{+}, 2^{+}, and 4^{+} states in ^{20}Ne. (See Figs. 4 and 5.) The error bars in these figures represent only the statistical error on the yield; the uncertainty in the absolute cross sections is about 20% and is dominated by the uncertainty in the target thickness. In the case of the ^{12}C target, at angles $\theta_{lab} \geq 100°$, the two members of the doublet could not be resolved, and only the sum of the yields $^{7}Be_{(0)} + {}^{7}Be_{(1)}$ was extracted. For those angles a value of $d\sigma_{(0)}/d\sigma_{(1)} = 2.0$ was used to extract separate cross sections for the $^{7}Be_{(0)}$ and $^{7}Be_{(1)}$ transitions; this value was arrived at as the average of the $d\sigma_{(0)}/d\sigma_{(1)}$ ratio for the 10 data points, $65° \leq \theta_{lab} \leq 85°$, immediately

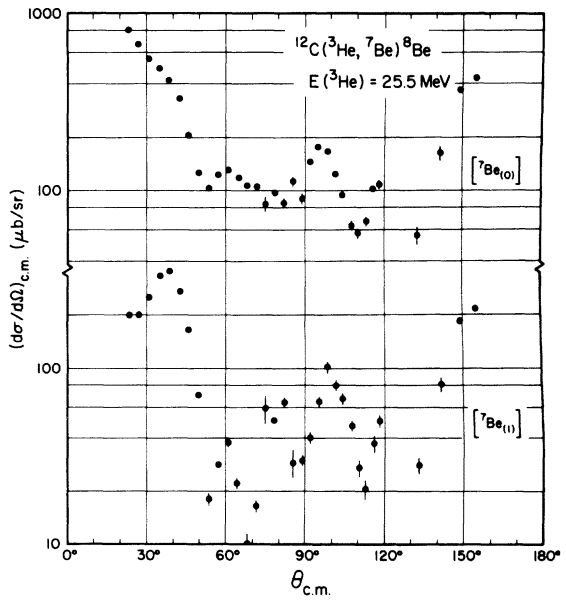

FIG. 4. Angular distributions for the ^{7}Be ejectile in its ground state (0) and its first excited state (1) for the ^{12}C(^{3}He, ^{7}Be)^{8}Be reaction at 25.5 MeV.

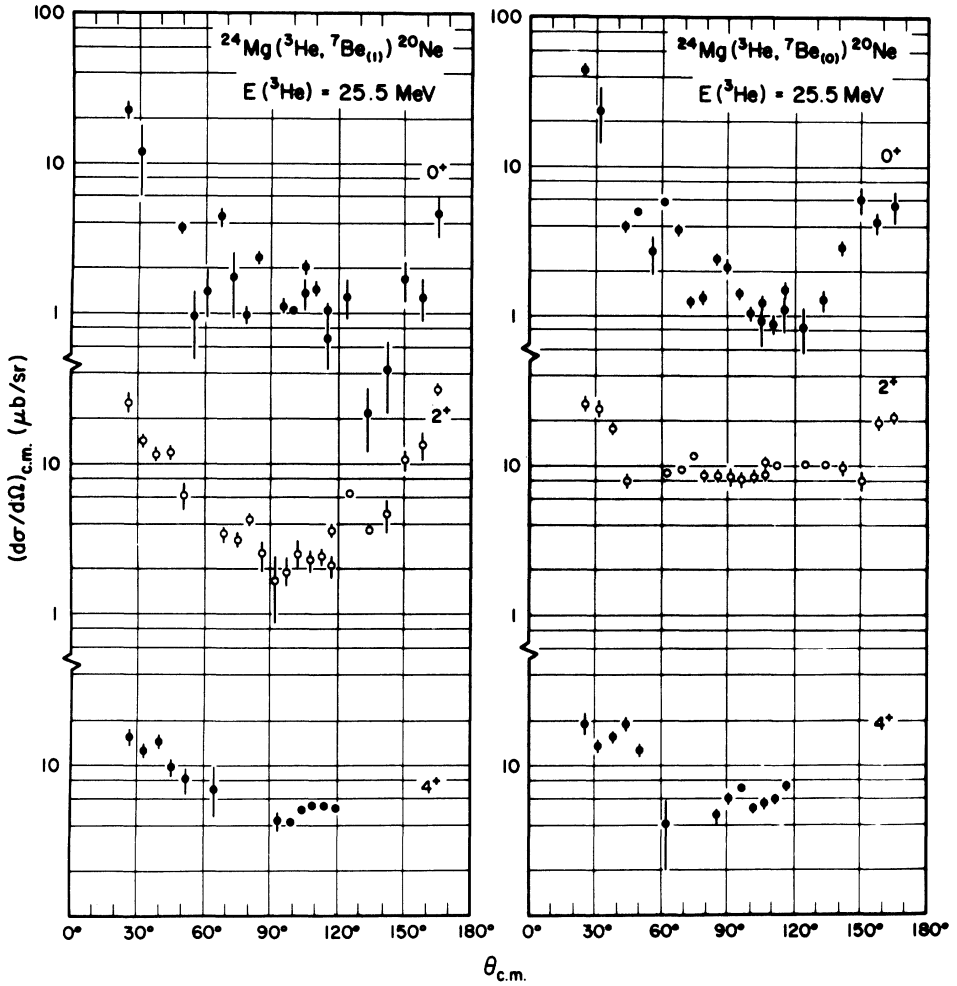

FIG. 5. Angular distributions for the ^{7}Be ejectile in its ground state (0) and its first excited state (1) for the ^{24}Mg(^{3}He, ^{7}Be)^{20}Ne reaction at 25.5 MeV.

preceding the $\theta_{lab} \geq 100°$ data. This value is also consistent with the value expected from the ratio of $(2J+1)_0/(2J+1)_1$.

At various angles, groups from the ^{16}O and ^{12}C contaminants interfered with the peaks in ^{24}Mg(^{3}He, ^{7}Be)^{20}Ne spectrum. A separate angular distribution was measured for the ^{16}O(^{3}He, ^{7}Be)^{12}C reaction under conditions identical to those for the ^{24}Mg(^{3}He, ^{7}Be)^{20}Ne angular distributions, and these data were then used to subtract the ^{16}O contaminant yields from the ^{24}Mg(^{3}He, ^{7}Be)^{20}Ne spectra. In cases where only one peak of a ^{24}Mg(^{3}He, ^{7}Be)^{20}Ne doublet was obscured by ^{16}O(^{3}He, ^{7}Be)^{12}C contaminant groups the area of the missing peak could be determined in this way. A separate ^{12}C(^{3}He, ^{7}Be)^{8}Be angular distribution was also measured under identical conditions; however, the application of this normalization and subtraction technique did not prove feasible for removing the ^{12}C(^{3}He, ^{7}Be)^{8}Be contaminant groups from the ^{24}Mg(^{3}He, ^{7}Be)^{20}Ne spectra. This failure was partially due to the difficulty in accurately handling the broad, 2.90-MeV first excited state in ^{8}Be and partially due to the much larger ^{12}C(^{3}He, ^{7}Be)-^{8}Be yields, with the subtraction of two large numbers resulting in statistically insignificant net differences.

IV. DISCUSSION OF EXPERIMENTAL RESULTS

The data presented in Fig. 5 suggest several comparisons that can be made. First note that all angular distributions are forward peaked with the $0^{+} \rightarrow 0^{+}$ transitions being the steepest at forward angles and also the most oscillatory. The angular distributions for transitions to higher-spin states in ^{20}Ne are less steep and show less structure than those to the ground state. This is a characteristic of angular distributions for the (^{3}He, ^{7}Be) reaction on other targets and suggests the

importance of direct-reaction contributions.

The rather complete angular range covered by the data at 25.5 MeV offers an opportunity to examine the reaction mechanism. The back-angle peaks immediately suggest a compound-nuclear reaction. Indeed, a study of cross correlations of the excitation functions of the $^{19}F(^3He, ^7Be)^{15}O$ and $^{19}F(^3He, ^7Li)^{15}N$ reactions by Dêtraz *et al.*[21] demonstrated the statistical nature of these reactions at $\theta_{lab} = 165°$. However, there are distinct problems with this hypothesis when applied to the $^{12}C(^3He, ^7Be)^8Be$ data. An exhaustive series of Hauser-Feshbach calculations (discussed below) failed to fit even the shape of the rise at forward and backward angles. As discussed below, the forward-angle data ($<50°$) can be satisfactorily fitted with a direct-reaction model assuming the transfer of an α-particle cluster; this then suggests that the backward peaking may be due to a direct-reaction process such as heavy-particle stripping or heavy-particle knockout. The very striking, sharp minima which persist in the data from 25.5 MeV up to at least 42 MeV[15,22,23] (Fig. 6) could then represent an interference between this direct process and the "normal" transfer process which peaks at forward angles. Calculations are under way to test this hypothesis.

While the $^{24}Mg(^3He, ^7Be)^{20}Ne$ angular distributions are also strongly forward peaked, the backward rise is not as extreme and generally is reasonably fitted by a Hauser-Feshbach calculation. The stronger forward rise is then evidence for some direct-reaction contribution, about which more will be said in Sec. V B in connection with the fitting of a direct-reaction model to this forward peak.

Additional information about the reaction mechanism can be extracted from a comparison of the

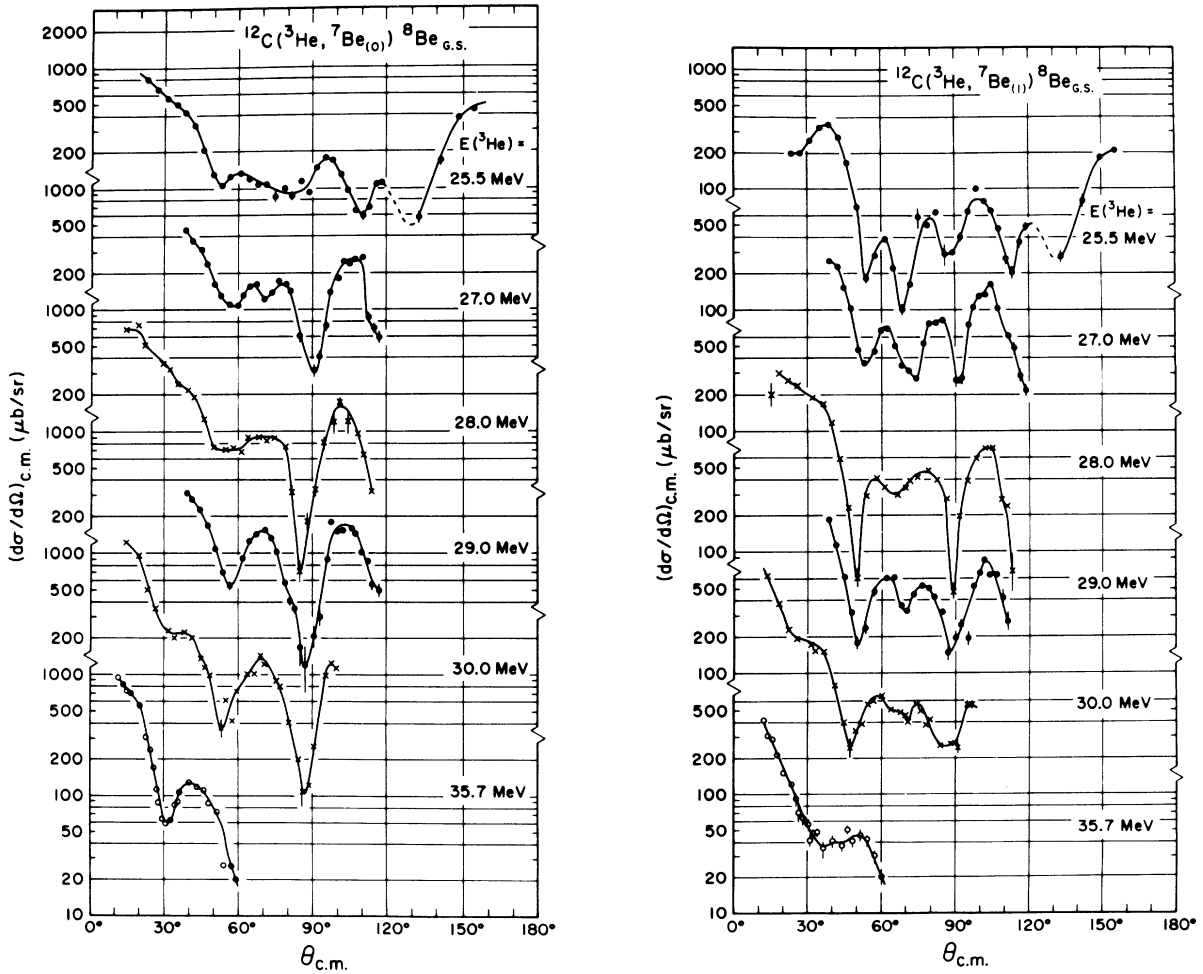

FIG. 6. Angular distributions for the ^7Be ejectile in the $^{12}C(^3He, ^7Be)^8Be$ reaction for several incident energies. Those at 25.5, 27.0, and 29.0 MeV are from this work; those for 28.0 and 30.0 MeV are from Ref. 15; and that at 35.7 MeV is from Ref. 22. The lines are to guide the eye.

angular distributions for $^{7}Be_{(0)}$ and $^{7}Be_{(1)}$ groups populating the same state in the final nucleus. There is considerable evidence[14,24] to suggest that these two states of ^{7}Be have the same spatial wave function and are split only by a small spin-orbit force. In the cluster model they are just a ^{3}He and a ^{4}He in a relative P state with a spin-orbit coupling of $\frac{3}{2}^-$ and $\frac{1}{2}^-$, respectively. If we assume that the transfer reaction proceeds via a direct mechanism and that there are no spin-dependent forces, then the angular distributions for the ground and first excited states of ^{7}Be should be identical in shape and be related in magnitude simply by the ratio of $(2J+1)$, i.e., 2:1. The extent to which the data do or do not follow this simple relationship is an indication of the validity of the above assumptions. At center-of-mass angles less than 30° (where direct-reaction effects might be expected to dominate any compound contributions) the transitions reported by Détraz *et al.*[15] and those which we have studied in the present experiments almost universally show a cross section ratio of 2:1, in agreement with this expectation. At more backward angles the ratio fluctuates from 6:1 to 1:2 in some cases, due to strong oscillations which are not quite in phase. In general, however, the $^{7}Be_{(0)}$ and $^{7}Be_{(1)}$ angular distributions are quite similar in shape, and their cross sections have a ratio between 0.7:1 and 3.0:1. The ^{20}Ne (2^+) angular distributions are quite anomalous in this respect, having distinctly different shapes and cross section ratios in the range 0.7:1 to 5.0:1. Other examples of such dissimilar behavior have been reported previously for the (^{3}He, ^{7}Be) reaction on other targets.[15,25] In these cases it is not possible to determine which of the assumptions noted above is not valid, but it is interesting to note that the direct-reaction calculations discussed below match the data best at the forward angles where the ratio of $^{7}Be_{(0)}$ to $^{7}Be_{(1)}$ is approximately 2:1.

We may gain further insight into the reaction mechanism by examining the spectra and noting which states are excited. Unfortunately, for the ^{12}C and ^{16}O targets the energies of ^{7}Be were too low to allow the observation of anything but the first two states at all but the most forward angles. For the ^{24}Mg target, however, states up through 6 MeV are visible at $\theta_{lab} \lesssim 100°$. The absence of the 2^- unnatural parity state at 4.97 MeV in the 90° spectrum (Fig. 7) is consistent with the observations of Steele, Crawley, and Maripuu[26] for the $^{24}Mg(^{3}He, ^{7}Be)$ reaction at $E(^{3}He) = 70$ MeV and with those of McGrath *et al.*[27] and of Comfort *et al.*[28] for the $^{24}Mg(d, ^{6}Li)^{20}Ne$ reactions; all of these authors report only weak population of this 2^- state at forward angles. Unfortunately we were not sensitive to the 2^- at more forward angles in the present experiment due to the large background from ^{12}C contamination of the ^{24}Mg targets. Note also in Fig. 7 that the 3^- state at 5.62 MeV (which is the next member of this $K^\pi = 2^-$ band) is strongly excited, while there is no evidence for the population of the 1^- state at 5.79 MeV. This situation is reversed from that found for the (^{6}Li, d) and (^{7}Li, t) reactions leading to ^{20}Ne final states. This reversal can be understood from the intrinsic structure of these states. The 3^- state, as the second member of the $K^\pi = 2^-$ rotational band built on the 2^- state at 4.97 MeV, is believed to have a $(0p)^{-1}(1s0d)^5$ structure,[29] while the 1^- state at 5.79 MeV is the bandhead of a $K^\pi = 0^-$ rotational band with a $(1s0d)^3(1p0f)^1$ intrinsic structure. Hence, based on a simple one-step, direct-re-

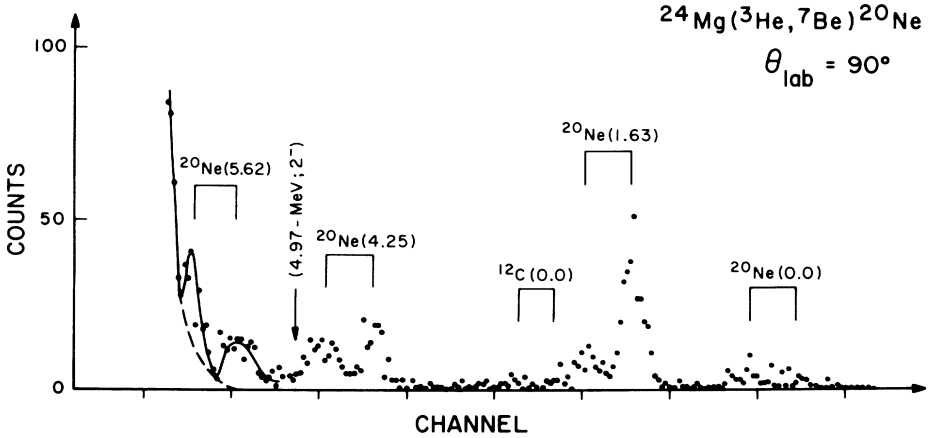

FIG. 7. Energy spectrum of ^{7}Be particles emitted in the (^{3}He, ^{7}Be) reaction at 90° from a ^{24}Mg target at 25.5 MeV. The expected position of the 2^- state at 4.97 MeV in ^{20}Ne is indicated. The doublet labeled $^{12}C(0.0)$ is from the (^{3}He, ^{7}Be) reaction on ^{16}O contaminants. The cutoff at low channels results from ^{7}Be stopping in the ΔE detector.

action mechanism and starting from a predominantly $(1s0d)^8$ ^{24}Mg ground state the $(0p)^{-1}(1s0d)^5$ $K^\pi = 2^-$ band is clearly much more easily accessible via a four-nucleon-pickup reaction than the $(1s0d)^3(1p0f)^1$ $K^\pi = 0^-$ band. Similarly, starting from a $(0p)^{12}$ closed shell ^{16}O ground state a four-nucleon-stripping reaction will preferentially populate the $K^\pi = 0^-$ band rather than the 2^- band. Population of the "unpreferred" band can occur, of course, via multistep direct reactions, compound-nuclear reactions, other components in the wave functions of the target ground states, etc. These mechanisms can only be sorted out through a thorough measurement and analysis of the angular distribution of these states. Since the $K^\pi = 2^-$ band can be preferentially populated via a simple one-step direct mechanism in the ^{24}Mg(^{3}He, ^{7}Be)^{20}Ne reaction, the absence of the 2^- member of that band in Fig. 7 can be used to set upper limits on the contributions from these other mechanisms even though we were not able to measure a detailed angular distribution for this state.

V. CALCULATIONS

A. Compound nuclear

In order to investigate the importance of statistical compound-nuclear processes in the reactions studied, a series of Hauser-Feshbach calculations was carried out using the code STATIS.[30] For the calculations on the (^{12}C + ^{3}He) system and for those on the (^{24}Mg + ^{3}He) system the p, n, d, ^{3}He, α, and ^{7}Be channels were included since these channels have the highest center-of-mass decay energies from the compound nucleus. The single most important parameter in these calculations is the density of levels in each channel; this parameter and the Q value determine how the flux is dis-

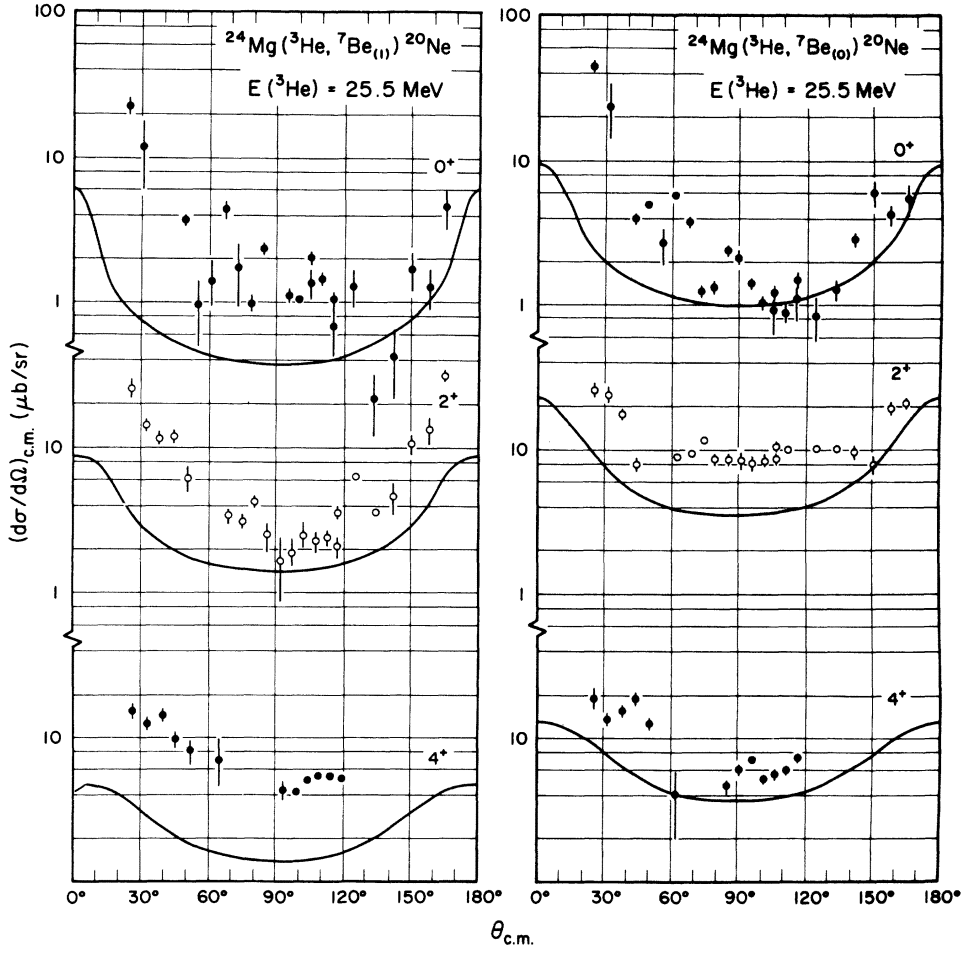

FIG. 8. Hauser-Feshbach calculations for the six angular distributions measured for the ^{24}Mg(^{3}He, ^{7}Be)^{20}Ne reaction. The curves have a normalization of 0.32 and correspond to normalizing the calculation for the 2^- (4.97 MeV) state to an upper limit of 1 μb/sr at $\theta_{lab} = 90°$.

tributed among the channels. The level density parameters were taken from Hanson's compilation[31] of those values which best fitted the available data. Several sets of optical potentials were tried, but the results were relatively insensitive to them. Details of the calculations are available elsewhere.[32]

A modified yrast cutoff was applied for all calculations; that is, the compound nucleus was assumed to be formed only for those l values in the entrance channel which are below the yrast level and for which the transmission coefficients are greater than 0.5. The first criterion insures that the compound nucleus does not have more angular momentum than it can support, while the second assures that there is a reasonable probability that the two nuclei in the entrance channel "come close enough" for the compound nucleus to be formed. The limit of 0.5 on the transmission coefficients is arbitrary; variations of the cutoff angular momentum by a few units in either direction make at most a factor of 2 difference in the flux in the ^{7}Be channel.

In general, the calculations predicted cross sections which were a factor of 2–10 too large. Any realistic change in the input parameters could not produce more than a factor of 2 change in the overall normalization. The absolute normalization of the calculation was therefore adjusted (a factor of 0.32) to fit the measured upper limit of 1.0 μb/sr for the cross section to the 4.97-MeV (2^-) state at $\theta_{lab} = 90°$; the relative normalizations for all of the other states were then taken as determined by the calculation. For the other negative parity states in Fig. 7, this procedure gives a prediction which is less than the measured cross section for the 5.62-MeV (3^-) state (a state which is expected to be populated via both compound and direct routes) and predicts a cross section for the 5.79-MeV (1^-) state which is below our experimental upper limit for that state, consistent with hypothesis that it would be populated only via compound-nuclear reactions. The results for the $K^\pi = 0^+$ ground-state band are shown in Fig. 8. In general the agreement between the calculation and these data is quite reasonable for angles $\theta_{c.m.} \geq 90°$. The 2^+ $^7Be_{(0)}$ calculation misses the 90° region but does pick up the backward rise. The 4^+ $^7Be_{(1)}$ result looks like it should be higher, but nothing could be done to bring this curve up without distrubing the normalizations of the other curves.

It should be noted that the Hauser-Feshbach results are energy-averaged cross sections and that the data were taken only at a single bombarding energy. However, the target was approximately 10 keV thick to the entering beam, and the compound nucleus ^{27}Si is being formed at an excitation energy of 36 MeV at which energy the density of levels is believed to be much greater than 5.0 keV^{-1}, so that an energy averaging is taking place in the experiment. These results then seem to indicate that at angles backward of 90° statistical compound-nuclear processes are contributing significantly to the ^{24}Mg(^{3}He, ^{7}Be)^{20}Ne cross sections.

The situation for the ^{12}C(^{3}He, ^{7}Be)^{8}Be reaction is not as simple as that for the ^{24}Mg(^{3}He, ^{7}Be)^{20}Ne reaction, since there are no low-lying unnatural parity levels in ^{8}Be to determine an upper limit to the statistical-compound contribution. Although similar results were obtained for all energies, only the calculations for 25.5 MeV, where there exist back-angle data, will be discussed. Figure 9 shows the results of a calculation with an angular momentum cutoff of 9.5 in the entrance channel and a normalization factor of 0.15 to 0.10 applied so that the curve approximated the average cross section around 90°. A higher constant could have been applied so that the Hauser-Feshbach result would go through some of the back-angle points, but it was felt that it was unreasonable, since the calculation would then grossly overestimate the data in the region around 90° and since the shapes of the calculated curves do not really match those of the data in the back-angle region anyway. The results for the ^{12}C(^{3}He, ^{7}Be)^{8}Be reaction seem to point to there being a significant

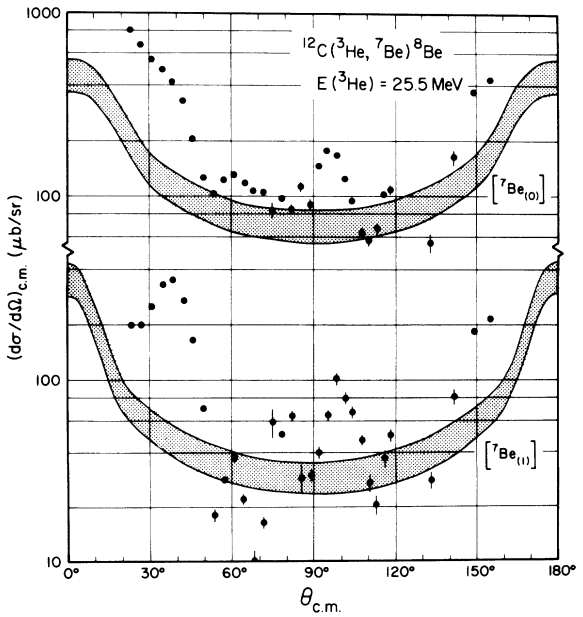

FIG. 9. Hauser-Feshbach calculations for the ^{12}C(^{3}He, ^{7}Be)^{8}Be angular distributions. The curves define a band of normalizations from 0.10 to 0.15.

direct component to the cross section at both forward angles and backward angles.

B. Finite-range DWBA and coupled-channels Born-approximation analyses

As is evident from the above discussion, there is significant direct-reaction contribution to the angular distributions at forward angles. Paper I[33] of this series emphasized the importance of using a finite-range DWBA model for calculating direct-reaction cross sections in α-particle-transfer reactions where the relative motion between the α particle and the core of the projectile is a non-S state, e.g., (^{3}He, ^{7}Be) and (^{7}Li, t) reactions. It also showed the importance of including multistep processes and transfer from excited states when the target or residual nucleus is deformed. The code FRIMP, described in Paper I, was written to do such calculations and has been used exclusively in the work described below.

All calculations were done assuming a cluster model for the target nucleus and the ^{7}Be ejectile. The quantum numbers of the bound state wave functions were fixed by assuming that all energy was contained in the relative motion of the α particle and the core. Two different radial forms of the bound state wave functions were tried. Several DWBA calculations were made using the solution to a Woods-Saxon well with a diffuseness of 0.65 fm and radius parameters in the range 1.00 to 1.25 fm (where these parameters are related to the radius by $r = r_0 A_{\text{core}}^{1/3}$) for both the target nucleus and the ^{7}Be. These variations did not make significant changes in the shapes of the calculated angular distributions but did modify the height of the rise at forward angles and the overall magnitude of the cross section. The rms radii of the bound state wave functions were calculated using the relation $\langle r^2 \rangle = \int \psi^* r^2 \psi \, d^3r$ and were compared to the tabulated results obtained from electron scattering.[34] A radius parameter in the range 1.0 to 1.1 fm seems to give the best agreement with these tabulated results. The second radial form was a harmonic oscillator wave function smoothly matched to a tail of the correct binding energy. The size parameter ν was varied from its initial cluster model value[35] of $4(A-4)A^{-4/3}$ fm^{-2}, in order to arrive at an rms radius as explained above; generally not much change was needed to achieve this. Because the harmonic oscillator wave function had more flux in the interior region than a Woods-Saxon wave function of the same rms radius, there were some differences between DWBA calculations performed with these two types of wave functions. All of the calculations shown below were done with the harmonic oscillator plus tail form because they seemed to give a slightly better agreement with the data. These parameters are summarized in Table I.

In all of the calculations that follow, a post approximation was used, and the "stripping" interaction was taken to be simply V(^{3}He-^{4}He), the potential that binds the ^{3}He and α clusters in the ^{7}Be nucleus. The validity of omitting the Coulomb terms from the interaction potential was checked by carrying out a calculation for the ^{12}C(^{7}Li, t)^{16}O reaction in which the full set of Coulomb terms was included. A comparison between the results of this calculation and one in which the Coulomb terms were not included showed that the two calculations produced angular distributions with nearly identical shapes and with only a 3% difference in absolute magnitude. This is consistent with the results reported earlier by DeVries[36] in a study of stripping interactions for multinucleon transfer calculations.

1. ^{24}Mg(^{3}He,^{7}Be)^{20}Ne reaction

This reaction appeared to be a good candidate in which to investigate the effects of multistep processes. It is well known that both ^{24}Mg and ^{20}Ne are deformed in shape and have enhanced transition strength in their ground-state bands. A recent SU_3 calculation[37] of the α structure of ^{24}Mg predicts a strength for the direct pickup to the ^{20}Ne 2^+ state which is 0.13 times weaker than that for the ground-state to ground-state transition. Hence, it seemed likely that second-order effects could compete with this direct route. Below we compare the results of DWBA and coupled-channels Born-approximation calculations for this reaction.

The optical model parameters for the ^{3}He + ^{24}Mg channel were taken from a study of ^{3}He scattering at 24 MeV.[38] Since the present analysis does not permit the use of spin-orbit forces in the distorted waves, the small spin-orbit term found in the above reference was dropped; the recalculated fit was found to be nearly as good as that with the spin-orbit term. For the CCBA calculations these same scattering data were refitted with a coupled-

TABLE I. Bound state parameters for harmonic oscillator plus tail wave functions.

Nucleus	N $(2n+l)$	l	ν (fm^{-2})	rms radius (fm)
^{24}Mg = ^{20}Ne$\otimes\alpha$	8	0, 2, 4	1.1	2.98
^{12}C = ^{8}Be$\otimes\alpha$	4	0, 2	1.0	2.45
^{7}Be = ^{3}He$\otimes\alpha$	3	1	1.2	2.45

TABLE II. Optical model parameters used in transfer calculations.

System	V (MeV)	r_0 (fm)	a (fm)	W (MeV)	W_D (MeV)	r_{0I} (fm)	a_{0I} (fm)	r_{0c} (fm)	β_2
$^{24}Mg + ^{3}He$									
Set I	152.8	1.15	0.746	•••	18.33	1.217	0.945	1.30	•••
Set II	172.8	1.20	0.640	•••	18.33	1.217	0.845	1.30	0.48
$^{20}Ne + ^{7}Be$									
Set III	197.5	1.009	0.878	•••	22.517	1.448	0.822	2.13	•••
Set IV	160.0	1.02	0.9	•••	16.0	1.60	0.80	2.20	0.56
$^{12}C + ^{3}He$									
Set V	169.0	1.14	0.675	32.1	•••	1.82	0.566	1.40	•••
Set VI	169.0	1.14	0.675	21.8	•••	1.82	0.566	1.40	−0.54
$^{8}Be + ^{7}Be$									
Set VII	50.0	1.5	0.834	4.0	12.0	1.86	0.802	2.5	•••

$$U(r) = V_c - (V + iW) f(x) + 4iW_D \frac{df(x_I)}{dr} ,$$

where

$$V_c = Z_1 Z_2 e^2 \begin{cases} 1/r & r > R_c \\ \left(3 - \frac{r^2}{R^2}\right) \Big/ 2R_c , & r \le R_c \end{cases} , \quad R_c = r_{0c} A^{1/3} ,$$

$$f(x) = (1 + e^x)^{-1} ; \quad x = \frac{r - r_0 A^{1/3}}{a} .$$

channels program (by manually changing the parameters—this was *not* a search code) which included scattering to the 1.36-MeV 2^+ state explicitly. The fit obtained in coupled channels was better than the original single-channel calculations of the elastic and inelastic scattering. As a check on the convergence of the coupled-channels procedure, a calculation was performed in which the 4^+ was also included. While no data were available for the 4^+ angular distribution, the fits to the 0^+ and 2^+ changed little (in the region of the available data) from the calculation which included only the 0^+ and 2^+. All optical potentials are summarized in Table II.

For the DWBA calculations, the ^{7}Be-^{20}Ne optical potentials were taken from a single-channel optical model analysis of $^{20}Ne + ^{7}Li$ elastic scattering at 38 MeV,[39] Set III in Table II. For the CCBA calculations, it was necessary to use an optical potential which did not implicitly include the effects of those inelastic channels which were being explicitly included in the coupled-channels formalism. Since a coupled-channels optical model analysis was not available for $^{20}Ne + ^{7}Li$ elastic scattering, the single-channel optical potential for $^{16}O + ^{7}Li$ elastic scattering[40] (Set IV in Table II) was chosen as the most suitable for the CCBA calculation.

Finite-range (FR) DWBA calculations of the 0^+, 2^+, and 4^+ states for both $^{7}Be_{(0)}$ and $^{7}Be_{(1)}$ are shown in Fig. 10. For reference the Hauser-Feshbach calculations discussed above are also shown. The shapes of the calculated angular distributions are in qualitative agreement with the data. They begin to deviate most strongly where the Hauser-Feshbach calculation becomes comparable in magnitude to the direct-reaction contribution. The calculations were normalized to the data to give the product of spectroscopic factors as defined in Paper I. Spectroscopic factors for the $^{24}Mg \rightarrow ^{20}Ne \otimes \alpha$ decomposition were arrived at by assuming a spectroscopic factor of 0.95 for the $^{7}Be \rightarrow ^{3}He \otimes \alpha$ decomposition. The resulting factors are summarized in Table III along with the SU_3 predictions of Draayer.[36] It is clear that the FRDWBA calculations greatly underestimate the cross sections to the 2^+ and 4^+ states, suggesting that indirect routes are enhancing the experimental cross sections.

Several finite-range CCBA calculations were made—all including both the 0^+ and 2^+ states in the entrance and exit systems. Including the 4^+ state in either channel would have been prohibitive from the standpoint of computer time and costs. As is evident from the formalism presented in Paper I, a CCBA calculation requires that the relative spectroscopic amplitudes be chosen before starting such a calculation. A set of amplitudes calculated with the SU_3 model was provided by Draayer[37] and is given in Table IV. CCBA

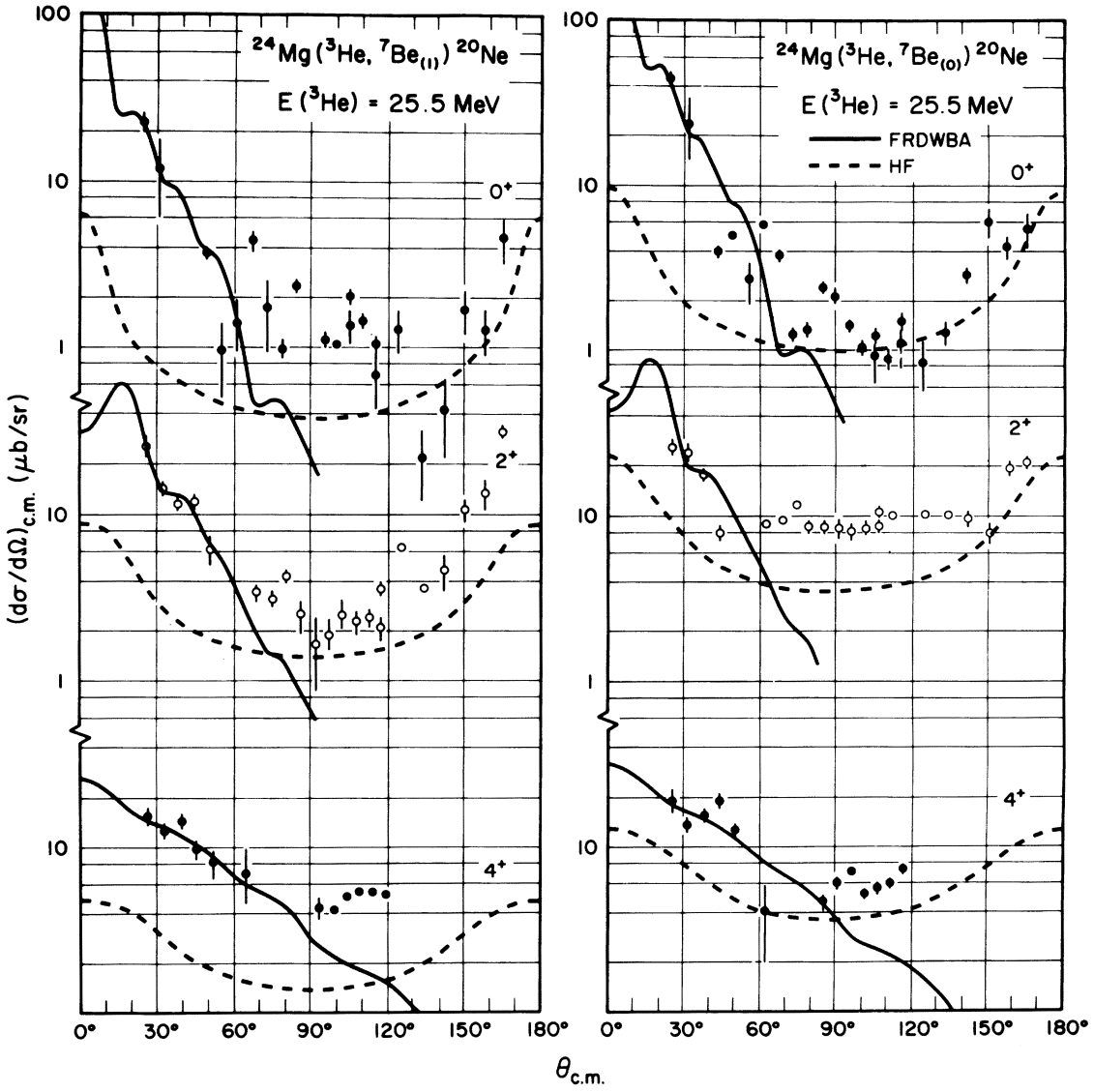

FIG. 10. Finite-range DWBA calculations for ^{24}Mg(^{3}He, ^{7}Be)^{20}Ne using the optical potential sets I and III and the bound state parameters of Table I. Hauser-Feshbach calculations are also shown.

calculations using these and potential Sets II and IV are shown in Fig. 11 for the 0^+ and 2^+ states. DWBA calculations using the same potential sets and wave functions are also shown. It must be emphasized that these are *not* the same optical potentials which were used in the DWBA calculations in Fig. 10. This set of modified DWBA calculations is included in Fig. 11 in order to separate the effects due to the explicit inclusion of the 2^+ inelastic channels from those effects which are due to the change in optical potentials. An absolute normalization of 1.2 was applied to *all* of the calculations in order to emphasize the differences in the *magnitude* of the cross sections calculated in the CCBA and DWBA analyses. Although still more cross section is needed, it is clear that the CCBA calculation does a better job in predicting the magnitude of the 2^+ angular distributions. A very significant improvement in the relative 0^+ to 2^+ cross sections can be realized if all of the parentage coefficients in Table IV are set equal to +1.0. While there are no theoretical justifications for such a change, it does indicate the direction in which the model must change if there is to be better agreement with the experimental data.

The improvement which can be obtained in the calculated strength of this transition by including coupled-channels effects in the analysis can be understood in light of the results presented in

TABLE III. Extracted spectroscopic factors from FRDWBA analysis of the $^{24}Mg(^{3}He,^{7}Be)^{20}Ne$ reaction.

		$^{7}Be_{(0)}$	$^{7}Be_{(1)}$	SU_3 model [a]
^{20}Ne	0^+	1.0 (0.67) [b]	1.0 (0.63) [b]	1.0
	2^+	15.4	23.4	0.13
	4^+	3.5	4.3	0.80

[a] Reference 37.
[b] Numbers in parentheses are absolute spectroscopic factors.

TABLE IV. SU_3 parentage factors used in the CCBA calculations.

$^{24}Mg(J^\pi) \rightarrow {}^{20}Ne(J^\pi) \otimes \alpha$	l value	SU_3 amplitude
$0^+ \rightarrow 0^+$	0	−0.457
$2^+ \rightarrow 0^+$	2	0.279
$0^+ \rightarrow 2^+$	2	−0.163
$2^+ \rightarrow 2^+$	0	0.279
	2	−0.007
	4	−0.338

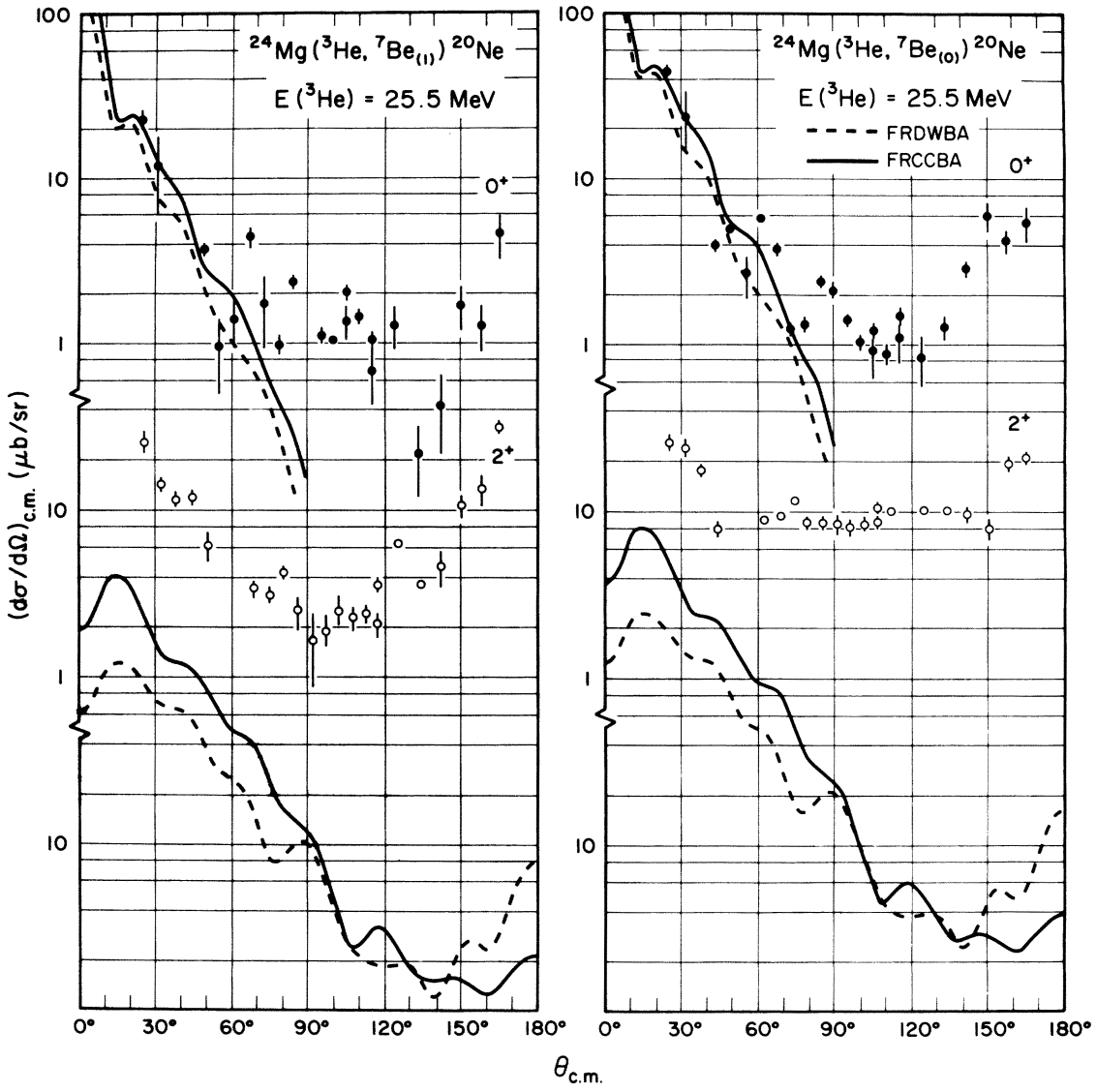

FIG. 11. Finite-range CCBA calculations for $^{24}Mg(^{3}He,^{7}Be)^{20}Ne$ using the optical potential Sets II and IV and the bound state parameters of Table I. The curves labeled FRDWBA are the results of calculations using the same parameters as the FRCCBA but with $\beta_2 = 0$. An overall normalization factor of 1.2 has been applied to all the curves.

Paper I.[33] There it was shown that the ground-state to ground-state transition dominated the calculation of the 2^+ cross section and that all other indirect routes are comparable in magnitude to the direct 2^+ route which would be calculated from the DWBA model alone. These results follow naturally from the relative size of the parentage factors and from the strength of the inelastic $0^+ \rightarrow 2^+$ transition in the final-state system. The importance of using a full coupled-channels treatment in such a situation cannot be overemphasized.

There are several factors which may contribute to the discrepancies between these calculations and the data. In view of the relatively strong one-step population of the 4^+ (4.25 MeV) state expected from Draayer's model[37] and in view of the strong inelastic coupling of the states in the ground-state band in ^{20}Ne, two-step transitions via the 4^+ state may play a very important role in populating the 2^+ (1.63 MeV) state. Unfortunately, however, the inclusion of this 4^+ state would make for a very expensive calculation. It is also known that the ^{24}Mg ground-state rotational band is not a pure (84) configuration, as has been assumed here. Akiyama, Arima, and Sebe[41] predict that approximately 25% of the wave function of ^{24}Mg consists of configurations other than (84), with (46) being the next largest component. A calculation including mixed configurations would be very costly at this time and cannot be justified in view of the other uncertainties in the calculation. Furthermore, our model for the direct transfer of a four-nucleon cluster, with inelastic effects in the target and residual nucleus but no spin-orbit forces in the distorted waves, cannot explain the differences in the measured ^{7}Be$_{(0)}$ and ^{7}Be$_{(1)}$ angular distributions. The calculations are very nearly identical for these two outgoing channels, except for a factor of 2 because of the spin multiplicity and small differences due to the slight change in binding energy and Q value. It is not clear where the model is wrong. It seems unlikely that the spin-orbit force (generally believed to scale as $1/A$) could be large enough for an $A = 7$ projectile to explain the observed difference in the measured ^{24}Mg(^{3}He, ^{7}Be)^{20}Ne(2^+) angular distributions. One possible explanation involves an interference between inelastic effects in the ^{7}Be nucleus and inelastic excitations in ^{20}Ne. Such an interference has been predicted for heavier ions.[42] An analysis of ^{7}Li scattering from a spherical target in which ^{7}Li$_{(0)}$ and ^{7}Li$_{(1)}$ are observed would help answer this question. There is considerable room for further theoretical and experimental work in understanding this reaction.

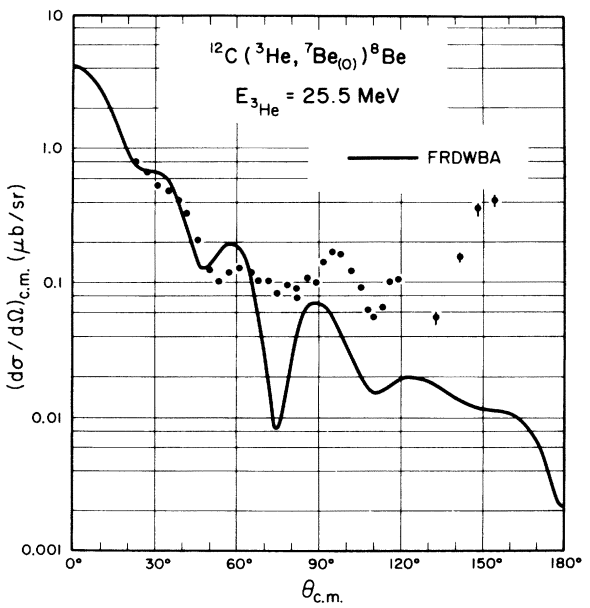

FIG. 12. Finite-range DWBA calculation of the ^{12}C(^{3}He, ^{7}Be$_{(0)}$)^{8}Be reaction at 25.5 MeV using optical potential Sets V and VII and the bound state parameters of Table I. A normalization factor of 18.4 has been applied to the curve.

2. $^{12}C(^3He,^7Be)^8Be$ reaction

Analysis of the ^{12}C(^{3}He, ^{7}Be)^{8}Be reaction proceeded along the same lines as that for the ^{24}Mg(^{3}He, ^{7}Be)^{20}Ne reaction. The ^{12}C ground state and first 2^+ state were assumed to consist of ^{8}Be in its ground state coupled to an $l = 0$ and $l = 2$ α particle, respectively. A macroscopic model was used to describe the excitation of the ^{12}C 2^+ state with $\beta_2 r_0 = -1.4$ (Ref. 43). For reasons of computational expediency, ^{8}Be was taken to be a spherical nucleus, with coupling to its 2^+ state taken into account only through the optical model.

Several sets of optical potentials were tried for both the ^{3}He and ^{7}Be channels[15,44-46]; all gave essentially similar results in the DWBA calculations. There was a problem in refitting the available ^{3}He inelastic scattering data in the coupled-channels analysis. This problem has been documented previously.[44] We did all our CCBA calculations with a set of potentials identical to that used in DWBA except that the volume absorption in the ^{3}He channel was reduced from 32.1 to 21.8 MeV in order to compensate for the explicit inclusion of the 2^+ channel in the calculation.

A typical DWBA calculation for the $E(^3\text{He}) = 25.5$ MeV data is shown in Fig. 12. The calculation does a reasonable job at fitting the data forward of $\theta_{c.m.} = 50°$ but fails at more backward angles. A spectroscopic factor of 18.4 was extracted from the fit. The same calculation was done for all of the angular distributions shown in Fig. 6; the fits

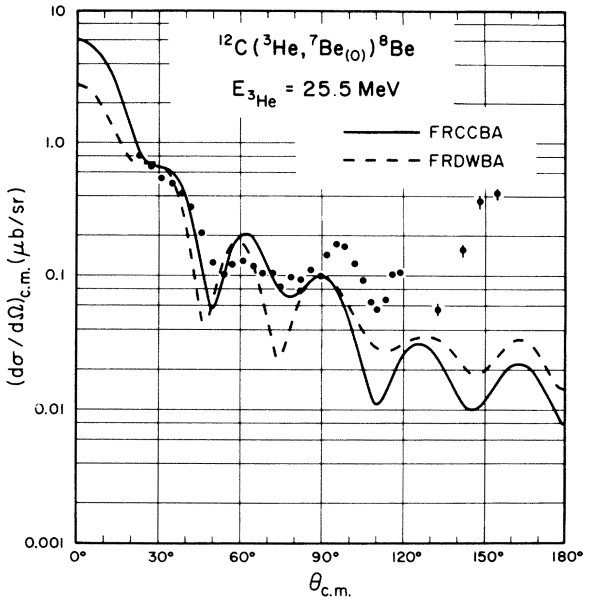

FIG. 13. Finite-range CCBA calculation of the $^{12}C(^3He,^7Be_{(0)})^8Be$ reaction at 25.5 MeV using optical potential Sets VI and VII and the bound state parameters of Table I. The curve labeled FRDWBA is the result of a calculation with the same parameters but with $\beta_2 = 0$. A normalization factor of 10.7 has been applied to both curves.

are qualitatively similar, and the extracted spectroscopic factors are surprisingly constant, lending some credence to the calculation procedure.

For the $^{12}C(^3He,^7Be)^8Be$ CCBA calculation, relative spectroscopic amplitudes are not available for the transition from $^{12}C^*$ (4.44 MeV, 2^+) to $^8Be_{g.s.}$, and therefore, the relative $2^+ \rightarrow 0^+$ to $0^+ \rightarrow 0^+$ amplitude was treated as a free parameter and was varied manually over the range ± 0.25 to ± 4.0. A good fit was obtained with this ratio set equal to -1.0; see Fig. 13. Also shown in Fig. 13 is a DWBA calculation ($\beta_2 = 0$) with the same potentials as used in the CCBA calculation. A normalization of 10.7 was applied to both curves in the figure. The inclusion of transfer through the 2^+ state enhances the forward-angle cross section and shifts the minima backward a few degrees. The CCBA calculation seems to be an improvement over the DWBA calculation of Fig. 12, although it still does not fit the backward data points.

Considerable effort was made to modify both the DWBA and CCBA calculations by varying the $^7Be + ^8Be$ optical potentials to reproduce the data at backward angles $\theta_{c.m.} \geq 50$. No combination of changes could make the calculations reproduce the sharp oscillations seen in the data at these angles. It is now felt that these oscillations, seen most clearly in the 25.5-MeV data, are due to the interference between two direct processes which have different angular dependence. One likely candidate is the transfer of a mass 5 cluster via the $^3He(^{12}C, ^7Be)^8Be$ reaction. This process is backward peaked relative the the "normal" four-particle transfer and would interfere with it; evidence exists for similar processes in other light-ion reactions.[47] However, the calculation of this process and its coherent addition to the four-particle-transfer amplitude requires modifications to the code FRIMP which are not anticipated at this time.

Recent work by Audi *et al.*[48] used a DWBA analysis of the (^3He, ^7Be) reaction to examine the variation of the α-particle-pickup spectroscopic factor for the ground states of $4N$ nuclei from ^{12}C to ^{40}Ca, except for ^{24}Mg. It was found that the relative spectroscopic factor $S_\alpha(4N)/S_\alpha(^{12}C)$ was insensitive to changes in the bound state radii and optical parameters. From our DWBA analyses we extract a relative spectroscopic factor $S_\alpha(^{24}Mg)/S_\alpha(^{12}C)$ of 0.04 in good agreement with the A dependence seen in the analysis[48] of the other relative spectroscopic factors $S_\alpha(4N)/S_\alpha(^{12}C)$.

VI. CONCLUSIONS

In general there is reasonable agreement between the finite-range DWBA and Hauser-Feshbach calculations described above and the (^3He, ^7Be) data, and meaningful relative spectroscopic factors having been extracted for α clustering in ^{12}C and ^{24}Mg. In the CCBA analysis, inelastic processes have been shown to make important contributions to these (^3He, ^7Be) transitions and to make significant changes in the absolute magnitudes of the extracted spectroscopic factors.

This work has been carried out to investigate the importance of FRCCBA and compound-nucleus contributions to these four-nucleon-pickup reactions. This is not a definitive or complete analysis. It is clear that further experimental and theoretical work is needed before this four-nucleon-pickup reaction is understood completely. In particular, the role of spin-orbit forces in the excitation of the ^7Be first excited state needs to be investigated before discrepancies between the $^7Be_{(0)}$ and $^7Be_{(1)}$ angular distributions can be resolved. It would also be helpful to have more data on excited states of nuclei in this and other regions of the Periodic Table so that multistep processes can be sorted out from the ambiguities of the ^7Be optical potential. Because of its much more negative Q value the (^3He, ^7Be) reaction is experimentally much more difficult to study than the (^7Li, t) reaction. However, the information provided by such a pickup reaction is complementary to the stripping results and is necessary for the complete understanding of clustering phenomena in

these nuclei. The (^{3}He, ^{7}Be) reaction appears to be a good α-particle-pickup reaction which can be used to extract meaningful relative spectroscopic factors.

VII. ACKNOWLEDGMENTS

The authors would like to thank Dr. Martin Cobern for his help in taking the data and in running some of the calculations. We are also grateful to Dr. Robert Ascuitto for his indispensable aid in interpreting the results of the calculations and to Dr. Jerry Draayer for sending us the results of his SU_3 calculation before their publication. We would also like to thank Dr. David Hanson for his assistance in doing the Hauser-Feshbach calculations.

---

*Work supported under U. S. E. R. D. A. contract E(11-1)-3074.

†Present address: Physics Department, Brookhaven National Laboratory, Upton, New York, 11973.

[1]K. Bethge, Annu. Rev. Nucl. Sci. 20, 255 (1970).

[2]A. A. Ogloblin, in *Nuclear Reactions Induced by Heavy Ions*, edited by R. Bock and W. R. Hering (North-Holland, Amsterdam, 1970), p. 231.

[3]R. Middleton, in *Nuclear Reactions Induced by Heavy Ions* (see Ref. 2), p. 263.

[4]K. Bethge, in *Nuclear Reactions Induced by Heavy Ions* (see Ref. 2), p. 277.

[5]A. Arima and S. Yoshida, Nucl. Phys. A219, 475 (1974).

[6]D. Kurath, Phys. Rev. C 7, 1390 (1973).

[7]A. Arima, V. Gillet, and J. N. Ginocchio, Phys. Rev. Lett. 25, 1043 (1970).

[8]K. Ikeda *et al.*, Prog. Theor. Phys. Suppl. 52, 1 (1972).

[9]H. Horiuchi and K. Ikeda, Prog. Theor. Phys. 40, 277 (1968).

[10]C. A. Barnes, Advan. Nucl. Phys. 4, 133 (1971).

[11]S. E. Koonin, T. A. Tombrello, and G. Fox, Nucl. Phys. A220, 221 (1974).

[12]G. Michaud and W. A. Fowler, Ap. J. 173, 157 (1972).

[13]R. G. Couch and K. C. Shane, Ap. J. 169, 413 (1971).

[14]T. A. Tombrello and P. D. Parker, Phys. Rev. 131, 2582 (1963).

[15]C. Détraz, H. H. Duhm, and H. Hafner, Nucl. Phys. A147, 488 (1970).

[16]C. Détraz, C. D. Zafiratos, C. E. Moss, and C. S. Zaidins, Nucl. Phys. A177, 258 (1971).

[17]J. P. Draayer (private communication).

[18]E. J. Rogers, Rev. Sci. Instrum. 32, 660 (1963).

[19]V. Radeka, Brookhaven National Laboratory Report No. BNL7448 (unpublished).

[20]P. D. Barnes, D. Biegelson, J. R. Comfort, and R. O. Stephen, Yale University Wright Nuclear Structure Laboratory Internal Report No. 25 (unpublished).

[21]C. Détraz, C. E. Moss, C. D. Zafiratos, and C. S. Zaidins, Phys. Rev. Lett. 26, 448 (1971).

[22]H. T. Fortune and B. Zeidman, in *Nuclear Reactions Induced by Heavy Ions* (see Ref. 2), p. 307.

[23]C. Zafiratos (private communication).

[24]D. Kurath, Phys. Rev. 101, 216 (1956).

[25]L. G. Keller, R. L. Kozub, and D. H. Youngblood, Texas A & M Cyclotron Laboratory Annual Report, 1972 (unpublished).

[26]W. F. Steele, G. M. Crawley, and S. Maripuu, Bull. Am. Phys. Soc. 18, 134 (1973); W. F. Steele, (private communication).

[27]R. L. McGrath, D. L. Hendrie, E. A. McClatchie, B. G. Harvey, and J. Cerny, Phys. Lett. 34B, 289 (1971).

[28]J. R. Comfort, W. J. Braithwaite, J. R. Duray, H. T. Fortune, W. J. Courtney, and H. G. Bingham, Phys. Lett. 40B, 456 (1972).

[29]T. K. Alexander, in *Proceedings of the Fifth Symposium on the Structure of Low-Medium Mass Nuclei, Lexington, Kentucky*, October 26–28, 1972, edited by J. P. Davidson and B. D. Kern (U. P. of Kentucky, Lexington, 1973), p. 272.

[30]R. Stokstad, Yale University Wright Nuclear Structure Laboratory Internal Report No. 52 (unpublished).

[31]D. Hanson (private communication).

[32]D. J. Pisano, Ph.D. thesis, Yale University, 1973 (unpublished).

[33]D. J. Pisano, Phys. Rev. C 14, 468 (1976) (preceding paper, Paper I).

[34]H. R. Collard, L. R. B. Elton, and R. Hofstadter, *Numerical Data and Functional Relationships in Science and Technology*, edited by K. H. Hellwege and H. Schopper (Springer-Verlag, Berlin, 1967), New Series, Vol. II.

[35]A. Arima, in *Dynamic Structure of Nuclear States, Proceedings of the 1971 Mont Tremblant International Summer School*, edited by D. J. Rowe, L. E. H. Trainor, S. S. M. Wong, and T. W. Donnelly (Univ. of Toronto Press, Toronto, 1972).

[36]R. M. DeVries, Phys. Rev. C 11, 2105 (1975).

[37]J. P. Draayer, Nucl. Phys. A237, 157 (1975); and (private communication).

[38]D. M. Patterson, J. S. Blair, J. G. Cramer, J. Eenmaa, and T. K. Lewellen, University of Washington Annual Report No. 104, 1972 (unpublished).

[39]M. E. Cobern, Ph. D. thesis, Yale University, 1974 (unpublished).

[40]M. E. Cobern, D. J. Pisano, and P. D. Parker, Phys. Rev. C 14, 491 (1976) (following paper, Paper III).

[41]Y. Akiyama, A. Arima, and T. Sebe, Nucl. Phys. A138, 273 (1969).

[42]R. J. Ascuitto (private communication).

[43]G. Satchler, Nucl. Phys. A100, 497 (1967).

[44]G. Ball and J. Cerny, Phys. Rev. 177, 1466 (1969).

[45]I. K. Oh, C. S. Zaidins, C. D. Zafiratos, and S. I. Hayakawa, Nucl. Phys. A178, 497 (1972).

[46]K. A. Weber, K. Meier-Ewert, H. Schmidt-Bocking, and K. Bethge, Nucl. Phys. A186, 145 (1972).

[47]R. M. DeVries, J. Perrenoud, I. Slaus, and J. W. Sunier, Nucl. Phys. A177, 258 (1971).

[48]G. Audi, C. Détraz, M. Langevin, and F. Pougheon, Nucl. Phys. A237, 300 (1975).

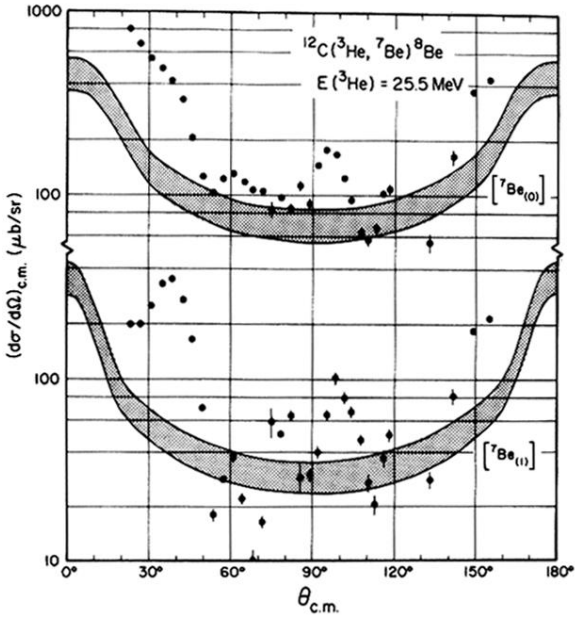

FIG. 9. Hauser-Feshbach calculations for the $^{12}C(^{3}He, ^{7}Be)^{8}Be$ angular distributions. The curves define a band of normalizations from 0.10 to 0.15.